Iranian Journal of Oil & Gas Science and Technology, Vol. 4 (2015), No. 4, pp. 15-32
http://ijogst.put.ac.ir

Minimizing Water Invasion into Kazhdumi Shale Using Nanoparticles

Aghil Moslemizadeh[1] and Seyed Reza Shadizadeh[2*]

M.S. Student, Department of Petroleum Engineering, Petroleum University of Technology, Ahwaz, Iran

Professor, Department of Petroleum Engineering, Petroleum University of Technology, Ahwaz, Iran

Received: August 22, 2014; *revised:* March 12, 2015; *accepted:* April 29, 2015

Abstract

Fluid invasion from water-based drilling mud (WBDM) into the shale formations causes swelling, high pressure zone near the wellbore wall, and eventually wellbore instability problems during drilling operations. For the stability of the wellbore, physical plugging of nanoscale pore throats could be considered as a logical approach toward avoiding the fluid invasion into the shale formation. This paper reports the effect of silica nanoparticles (NPs) as a physical sealing agent on the water invasion into Kazhdumi shale. To this end, pressure penetration apparatus was implemented. Typical WBDM in contact with Kazhdumi shale at different concentrations of NPs with different sizes was studied. The results indicated that the addition of NPs to the WBDM decreased water invasion into Kazhdumi shale. WBDM having 10 wt.% of 25 nm NPs reduced fluid invasion up to 72.76%.

Keywords: Fluid Invasion, Wellbore Instability, Nanoparticles (NPs), Physical Sealing Agent

1. Introduction

Wellbore instability is a major concern during drilling operations (Yu et al., 2003). Causes of wellbore instability problems can be divided into two categories, namely mechanical and physicochemical effects (Tan et al., 1996; Osuji et al., 2008). Mechanical effects, including drill string impacts on the wellbore wall, the difference in rock mechanics, and the redistribution of the forces around the wellbore (Zhu and Lui, 2013) are a direct result of drilling operations (Zeynali, 2012). These effects could be handled by affecting the circulating density through drilling/tripping practices and trajectory control (Lal and Amoco, 1999). Unlike the mechanical effects, the physicochemical effects are time dependent (Lal and Amoco, 1999; Osuji et al., 2008; Zeynali, 2012) and are a direct result of the interaction between the rock (especially shale) and drilling fluids.

Shales, fine grained sedimentary rocks, are allocated for about 75% of the drilled formation in oil and gas wells as well as the source of 90% of wellbore instability problems (Steiger and Leung 1992). These rocks have several characteristic, including a porosity varying from less than 1% to more than 50%, a low permeability from 10^{-6} to 10^{-12} Darcy, high clay content, and a laminated layer (Van Oort, 1994; Van Oort et al., 1996; Mody et al., 2002; Diaz-Perez et al., 2007). Non-clay minerals are

* Corresponding Author:
Email: shadizadeh@put.ac.ir

also present in shale, but they are generally considered inert, which only make contributions to physical properties such as density. Therefore, the swelling and dispersion characteristics of a particular shale are functions of the amounts and types of clay minerals present (Steiger, 1982). Among all the clays, sodium saturated smectites have enjoyed a lot of attention owing to high swelling potential and their occurrence frequencies during drilling operations (Anderson, 2010). Smectites clays have a negatively charged layer due to isomorphous substitution of the metal ions in the clay lattice, which is balanced by the sorption of cations in the region between the clay layers (Hill, 1982; Zhou et al., 1996; Anderson et al., 2010). The exposure of water sensitive shales to the conventional water-based drilling muds (WBDMs) results in their hydration and swelling due to the adsorption of water from WBDMs, which leads to a reduction in compressive strength (Chenevert, 1970), and eventually several problems during drilling operations. The common problems include tight hole, stuck pipe, high torque and drag, hole enlargement and washout, packing off hole fill, solid buildup in drilling fluids, and well control (O'Brien and Chenevert, 1973; Bol et al., 1994; Lomba et al., 2000). It has been reported that these problems could eventually lead to the suspension of the well prior to reaching the target (Tan et al., 1996). In the past, balanced activity oil-based muds (OBMs) were used for drilling through troublesome shale formations (Lomba et al., 1996), but environmental restriction (especially in offshore drilling) and high cost restrict their wide use (Mody et al., 2002). Therefore, the design and development of WBDMs with OBMs performance is currently an area of great interest within the industry.

It is widely accepted that extracting water out of shale could lead to shale strengthening and subsequently avoiding the shale failure owing to reducing the pore pressure. According to the Le Chatelier's principle, in the absence of other motivating forces, water tends to move from low salinity (high activity) region to high salinity (low activity) region (Fam and Dusseault, 1998). Osmosis is the flow of water from low salinity region to high salinity region across a membrane which allows water to move, but restricts the movement of ions (an ideal semipermeable membrane). In non-ideal semipermeable membranes, by the addition of water, some of the ions can move through the membrane. The membrane efficiency is a term to indicate the non-ideality of membrane systems. It is equal to one, zero, and between the one and zero for ideal, nonselective, and nonideal membranes respectively. It has been reported that shales could have a nonideal membrane behavior owing to their fine pore size and negatively charged clay surfaces (Van Oort et al., 1995; Van Oort et al., 1996; Lomba et al., 1996; Mody et al., 2002). The membrane efficiency of shales has been reported to be about 0.034 (an average of 63 data points), which is very small to the generation of an osmotic backflow of water from the formation toward the wellbore (when using high salinity mud) and also cannot overcome the flow of mud filtrate (AL-Bazali, 2011). Several experimental studies (Van Oort et al., 1995; Al-Bazali et al., 2006; Al-Bazali et al., 2007) indicated that the membrane efficiency of shales increased with an increase in the shale CEC, an increase in solute to pore size ratio, and a decrease in shale permeability. The low permeability characteristic of shales results in lack of formation of mud cake on the wellbore wall (Sensoy et al., 2009) and a slow flux of mud filtrate into the formation, leading to a significant pore pressure zone near the wellbore wall (van Oort, 2003) and subsequently wellbore instability. Therefore, physical plugging of nanoscale pore throats could be implemented to reach the several benefits, including pore pressure reduction owing to preventing the influx of mud filtrate toward the shale, shale swelling reduction owing to avoiding the more interaction between the shale and mud filtrate, the generation of high membrane efficiency due to shale permeability reduction, and consequently shale stability.

Silicates have a high potential to shale stability due to precipitation and gelation in shale pores, which results in a reduction in permeability and generating an osmotic membrane (Bailey et al., 1998). However, a number of disadvantages, including a high torque and drag due to precipitation of silica, health hazard at high pH values, and drilling fluid formulation restrict their wide use (Patel et al., 2007). The positive effects of nanoparticles (NPs) on the stability of Atoka, Golf of Mexico (Chenevert and Sharma, 2009; Sensoy et al., 2009) and Gurpi (Akhtarmanesh et al., 2013) shales have been demonstrated. The effect of NPs on the fluid invasion into Kazhdumi shale has not yet been reported in the literature. This work highlights the effects of silica NPs as a sealing agent on the fluid invasion into Kazhdumi shale.

2. Experimental

2.1. Materials

2.1.1. Nanoparticles.

In this study, two sizes of silica NPs were used. The specific properties of silica NPs used in this study are summarized in Table 1.

2.1.2. Shale sample

Kazhdumi shale, called Nahr Umr in the United Arab Emirates (Mehtal et al., 2010), with a green to brown color, the CEC value of 10 meq/100 g (determined via the methylene blue test) were extracted from the outcrop of Kazhdumi formation, Maghar strait, Khuzestan state, the southwestern of Iran. A large well-preserved shale sample was extracted from a depth of about 2 m and then sealed carefully after preparing several core plugs. To evaluate the swelling potential of Kazhdumi shale, 10 gr of crushed Kazhdumi shale with a particle size between 75 and 150 microns (between sieve mesh N.100 and N.200) was compressed under a pressure of 41 MPa for 30 min using a hydraulic compactor. The linear swelling curve of Kazhdumi shale exposed to tap water was determined at 60 °C using Ofite linear swellmeter, Houston, Texas. According to Figure 1, the linear swelling rate of Kazhdumi shale is 20.48% after about 2 hrs. The X-ray diffraction (XRD) analysis was implemented to determine the semiquantitative mineral composition of Kazhdumi shale. The XRD pattern and semiquantitative mineral composition are presented in Figure 2 and Table 2 respectively.

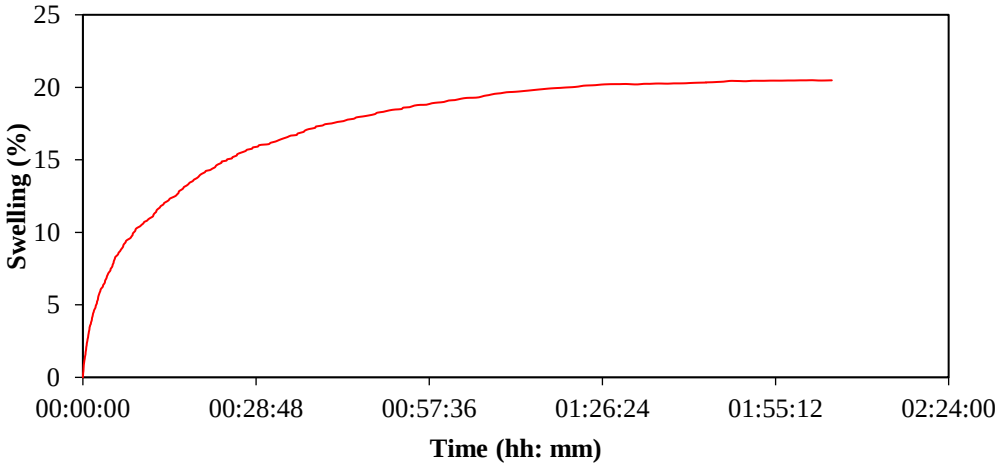

Figure 1
Swelling curve of Kazhdumi shale exposed to tap water at 60 °C.

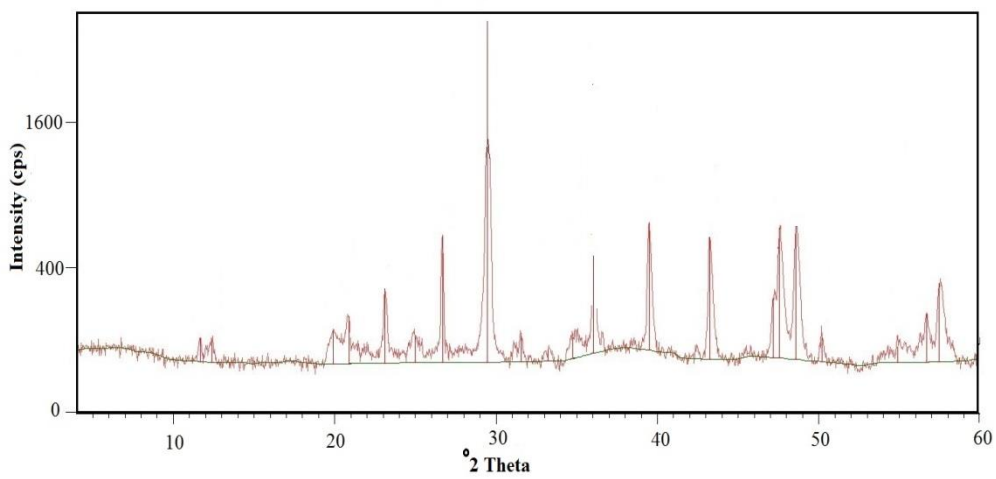

Figure 2
XRD pattern of Kazhdumi shale.

Table 1
Properties of silica Nanoparticles.

Typical particle size (nm)	Description	Color	Purity (%)	Surface area ($\frac{m^2}{g}$)	Solubility in water
10	Powder	White	99.5	560-690	Insoluble
25	Powder	White	99	180-600	Insoluble

Table 2
The semiquantitative mineral composition of Kazhdumi shale determined by XRD analysis.

Minerals	Weight Percentage (%)
Quartz	21
Calcite	46
Dolomite	1
Gypsum	3
Montmorillonite	12
Kaolinite	13
Illite	4

2.2. Methods and test procedure

2.2.1. Pressure penetration apparatus

In this study, a pressure penetration technique was implemented to investigate the shale membrane efficiency and physical plugging performance of nanoparticles. The main parts of the experimental apparatus (Figure 3) consist of a test cell (which withstands a maximum pressure and temperature of

100 MPa and 250 °C respectively), pumping system (high performance liquid pump (which supports volume rates ranging from 0.001 to 5 cm^3/min and pressures ranging from 0.1 to 40 MPa), accumulators, pressure sensors, and smart oven.

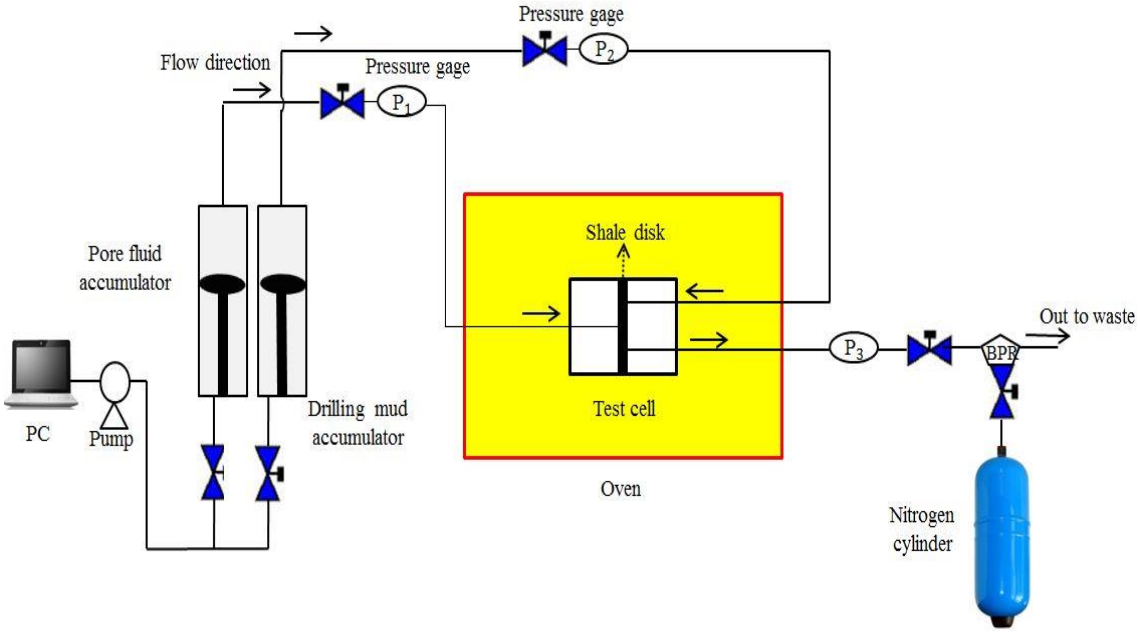

Figure 3
A schematic of the pressure penetration apparatus.

2.2.2. Shale disks preparation

According to the procedure of Sensoy et al. (2009), shale disks were prepared in a number of consecutive steps, including a) preparing several core samples from a large well-preserved Kazhdumi shale using an oil cooled coring bit with an inner diameter of 5.4 cm, b) placing each shale core sample in an acrylic plastic tube with an inner diameter of 6.35 cm, c) preparing 50/50 epoxy resin and pouring into the space between the shale core sample and the inner wall of the acrylic plastic tube, d) after curing the epoxy resin, slicing the shale sample with a thickness of 0.63 cm using an oil cooled circular saw, e) removing the acrylic plastic ring around the hardened epoxy resin, and f) immersing the prepared shale disks in a tank containing oil to prevent the interaction between the shale and atmosphere. It should be noted that epoxy resin, which is impermeable after hardening, was utilized to reach the shale disks diameter required for the test cell.

2.2.3. Shale water activity determinations

The shale, pore water, and mud activities must be similar to prevent any interactions between them (i.e. ion diffusion). Therefore, shale water activity (A_w) determination is very essential. Water activity is the ratio of the vapor pressure of water in a substance to the vapor pressure of pure water at the same temperature. The relative humidity of air is the ratio of the vapor pressure of air to its saturation vapor pressure. When vapor and temperature equilibrium are obtained, the water activity of the sample is equal to the relative humidity of air surrounding the sample in a sealed measurement chamber such as desiccator. Therefore, shale water activity could be determined in a sealed chamber by relative humidity measurements. This test was carried out in multiple steps, including placing a shale piece with a known weight in a desiccator with a known relative humidity, b) reweighting the

shale piece after a period of time, c) repeating this procedure using another relative humidity and new shale pieces until the weight difference of the shale piece before and after equilibrium (Δw) reached zero. Shale water activity is equal to the relative humidity at which the weight difference of the shale piece is zero. The flow chart of shale water activity determinations is presented in Figure 4.

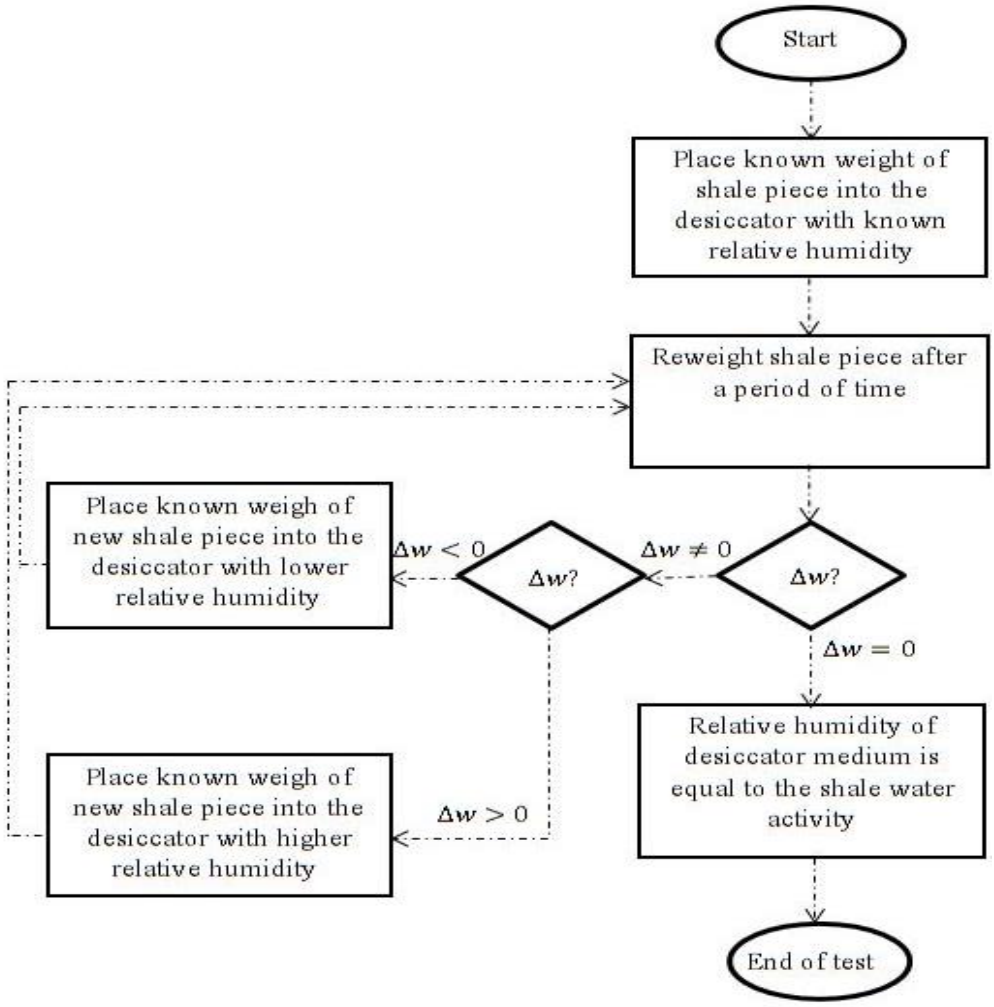

Figure 4
Flow chart of shale water activity determination.

2.2.4. Membrane efficiency tests

According to the aforementioned discussion, shales have a semipermeable membrane behavior. This positive aspect could be implemented to extract the water out of shale toward the wellbore, when using high salinity mud. Therefore, shale membrane efficiency determination is very essential. Shale membrane efficiency test was carried out by the simultaneous injection of pore fluid (which is herein referred to as an NaCl solution with a water activity of 0.93) from the pore fluid accumulator and the test fluid (which is herein an NaCl solution with a water activity of 0.85) from the mud accumulator into the both sides of shale disk at the same pressure of 0.27 MPa, by gradual increasing the test fluid pressure to a constant pressure (herein, 1.54 MPa), and finally by recording the pore pressure as a function of time. The test temperature was 25 °C. As addressed in several references (Akhtarmanesh et al., 2013; Van Oort et al., 1995), membrane efficiency can be determined by the following equations.

$$\Delta\pi = \frac{RT}{V} \times \ln \frac{A_{w,porefluid}}{A_{w,testfluid}} \quad (1)$$

$$\Delta\sigma = \frac{\Delta P}{\Delta\pi} \times 100 \quad (2)$$

where, $\Delta\sigma$ (%) is the membrane efficiency; ΔP (MPa) stands for the measured osmotic pressure; $\Delta\pi$ (MPa) represents the theoretical osmotic pressure; R and T are the gas constant and absolute temperature respectively; V denotes the partial molar volume of water; $A_{w,porefluid}$ and $A_{w,testfluid}$ are the water activity of pore fluid and the water activity of test fluid respectively.

2.2.5. WBDM design and properties determinations

In order to investigate the effect of silica nanoparticles on the fluid invasion into Kazhdumi shale, typical WBDM including different concentrations of nanoparticles was prepared. WBDMs containing nanoparticles were prepared by adding several common additives, including green starch and low viscosity poly anionic cellulose (PAC-LV) as fluid loss controllers, partially hydrolyzed polyacrylamide (PHPA) as a shale inhibition, XC-polymer as a viscosifier, sodium chloride as an activity adjustment, and potassium chloride as a shale inhibitor to the different concentrations of aqueous nanoparticle dispersion (prepared by Hielscher ultrasonic apparatus). The designed WBDM without nanoparticles was rolled at 93 °C for 16 hrs and its dial readings were recorded at 60 °C. The apparent viscosity, plastic viscosity, and yield point were calculated from 600 to 300 rpm dial readings using the following formula according to the API recommended practice of standard procedure for field testing drilling fluids (API, 1997).

$$AV = \frac{\varphi_{600}}{2} (cP) \quad (3)$$

$$PV = \varphi_{600} - \varphi_{300}\ (cP) \quad (4)$$

$$YP = \varphi_{300} - AV\ (Pa) \quad (5)$$

The viscometer was initially operated at 600 rpm for 10 seconds, and was then followed by a subsequent 10 second shut off. The maximum reading attained after starting rotation at 3 rpm is the initial gel strength (10-second gel) in pound per 100 square feet. The fluid sample was re-stirred at 600 rpm for 10 seconds, and after standing for another 10 minutes, the maximum reading after starting rotation at 3 rpm was recorded as 10-minuts gel strength in pound per 100 square feet. For the sake of the consistency, the gel strength was expressed in Pascal. The filter loss was measured in milliliters under a pressure of 0.7 MPa through a special filter paper (Baroid filter paper) for 30 minutes.

2.2.6. Pore plugging tests

Pore plugging tests were carried out as the procedure described for testing membrane efficiency. In this test, the test fluid referred to as WBDM contains different concentrations of nanoparticles. All pore plugging tests were performed at the mud pressure in the range of 1.44 to 1.86 MPa and at the pore pressure in the range of 0.37 to 0.55 MPa. The details of the test conditions are summarized in Table 3. The fractional reduction in pressure difference between the mud pressure and pore pressure

(both sides of shale disk) at the initial and plugging time (PT), which is the time required for plugging, of the tests can be calculated using the following equation:

$$\delta_j = \frac{\Delta P_{ij} - \Delta P_{pj}}{\Delta P_{ij}} \tag{6}$$

where, δ is the fractional reduction in pressure difference between the mud pressure and pore pressure at the initial and plugging times for different muds (j); ΔP_i (MPa) stands for the pressure difference between the mud pressure and pore pressure at the initial time; and ΔP_p (MPa) is the pressure difference between the mud pressure and pore pressure at the plugging time.

Therefore, the comparison between fluid invasion efficiency of the two tests, namely the test conducted using base mud and the one used base mud containing different concentrations of nanoparticles, can be obtained using the following equation:

$$\varepsilon = \frac{\delta_{WBDM} - \delta_{(WBDM+NPs)_{ii}}}{\delta_{WBDM}} \times 100 \tag{7}$$

where, ε (%) is fluid invasion reduction efficiency; δ_{WBDM} stands for the fractional reduction in pressure difference at the initial and plugging times for the base mud; $\delta_{WBDM+NPs}$ is the fractional reduction in pressure difference at the initial and plugging time for the base mud containing different concentrations (ii) of nanoparticles.

Table 3
Pore plugging tests conditions.

Test Number	**1**	**2**	**3**	**4**	**5**	**6**	**7**
Mud type	WBDF	WBDF + 10 nm nanoparticles			WBDF + 25 nm nanoparticles		
Mud A_w	0.93	0.93			0.93		
NPs (wt.%)	0	2	5	10	2	5	10
Pore fluid	Brine	Brine	Brine	Brine	Brine	Brine	Brine
Pore fluid A_w	0.93	0.93	0.93	0.93	0.93	0.93	**0.93**
T (°C)	60	60	60	60	60	60	**60**

3. Results and discussion

3.1. Shale water activity determinations

The percentage of weight difference ((Δw/ initial weight) × 100) of shale pieces versus water activities are presented in Figure 5. According to this figure, Kazhdumi shale water activity is equal to 0.93, at which the percentage of weight difference is zero. This activity was utilized as a guideline in the membrane efficiency and pore plugging tests.

3.2. Membrane efficiency tests

The result of membrane efficiency test is presented in Figure 6. As can be seen, pore pressure curve displays three different regions including transient (within the first 4 hrs), pseudo-plateau (in the next

8 hrs), and plateau (after the first 16 hrs) respectively. In the transient region, pore pressure increases sharply owing to the applied test fluid pressure being much greater than the osmotic pressure. It should be noted that the generation of osmotic pressure is due to the difference in water activity between the test fluid (NaCl solution with a water activity of 0.85) and pore fluid (NaCl solution with a water activity of 0.93). Pore pressure build up rate decreases sharply (pseudo-plateau region) with a decrease in the difference between the test fluid pressure and pore pressure, and eventually reached zero in the plateau region.

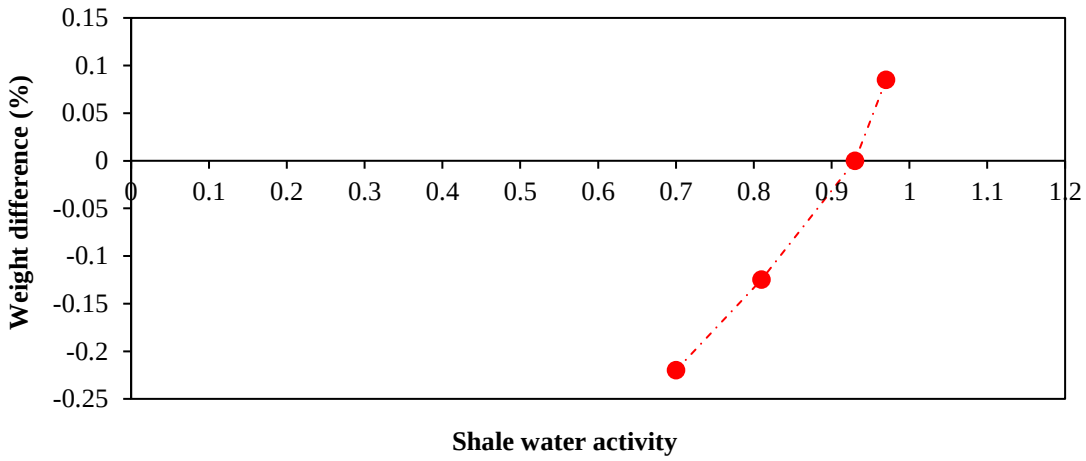

Figure 5
Results of shale water activity determinations for Kazhdumi shale.

The test fluid does not contain a sealing agent, so it can certainly be inferred that the constant difference between the test fluid pressure and pore pressure (in the plateau region) is related to the osmotic pressure. Therefore, this constant difference could be considered as the measured osmotic pressure (0.2133 MPa). By the implementation of Equation 2, the membrane efficiency of Kazhdumi shale can be obtained to be about 1.8%. This suggests that Kazhdumi shale should have a low membrane efficiency, which denotes that the osmosis phenomenon is an unreliable mechanism for describing the stability of Kazhdumi shale. Consequently, minimizing the water invasion into Kazhdumi shale using physical plugging of pore throats is highly essential for the stability of Kazhdumi shale.

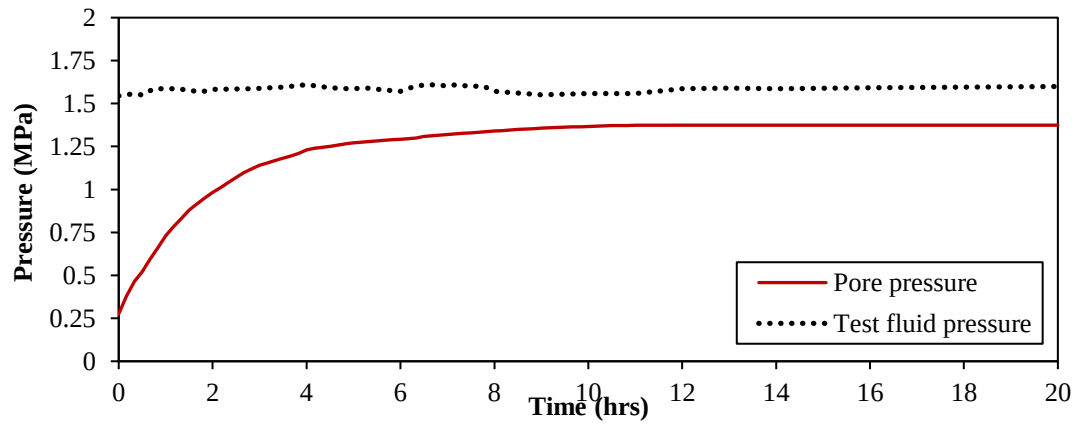

Figure 6
Results of membrane efficiency test with an NaCl solution (water activity=0.85) in contact with Kazhdumi shale.

3.3. WBDM properties determinations

The properties of WBDM without nanoparticles are presented in Table 4. This mud has desirable rheological properties and filtrate loss. In order to avoid the interaction between the mud, pore fluid, and shale sample, the activity of WBDM was tuned to be 0.93 (Kazhdumi shale water activity).

Table 4
Properties of designed WBDM without nanoparticles after being rolled at 93 °C for 16 hrs and reading at 60 °C.

WBDM properties	Value
θ_{600}	63
θ_{300}	45
Gel 10- sec (Pa)	4
Gel 10- min (Pa)	6
AV (cP)	31.5
PV (cP)	18
YP (Pa)	13.5
API Fluid Loss (ml/30 min)	4
MW (kg/m^3)	1041.2
A_w	0.93
pH	8.5

3.4. Pore plugging tests

Seven WBDMs containing different concentrations, namely 0, 2, 5, and 10 wt.%, of nanoparticles with two sizes of 10 nm and 25 nm were studied to evaluate the effect of nanoparticles on the water invasion into Kazhdumi shale. The pressure results are presented in Figure 7 for the base mud, in Figure 9 (a-c) for the base mud containing different concentrations of 10 nm nanoparticles, and in Figure 10 (a-c) for the base mud having different concentrations of 25 nm nanoparticles. In order to obtain a higher resolution in ε calculations for each test, the pressure data, including initial mud pressure (IMP), initial pore pressure (IPP), plugging pore pressure (PPP, a pore pressure at which plugging occurs), plugging mud pressure (PMP, the mud pressure at which plugging occurs), and δ_j are summarized in Table 5.

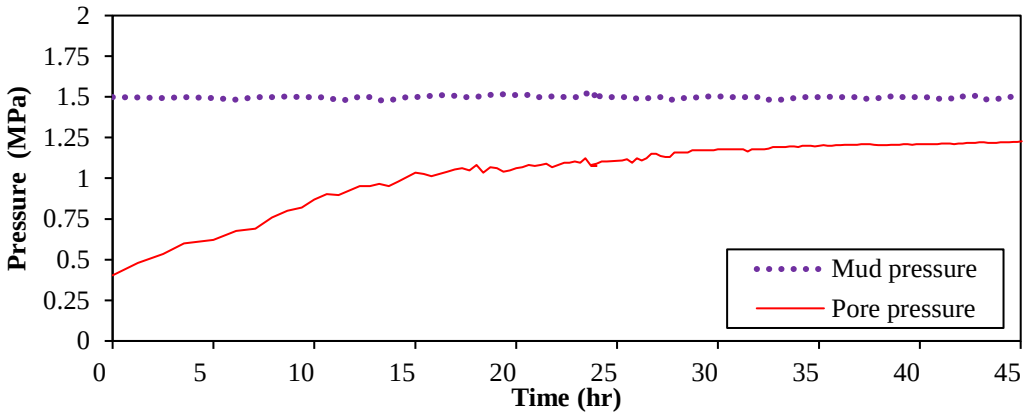

Figure 7
Results of pore plugging test of WBDM in contact with Kazhdumi shale.

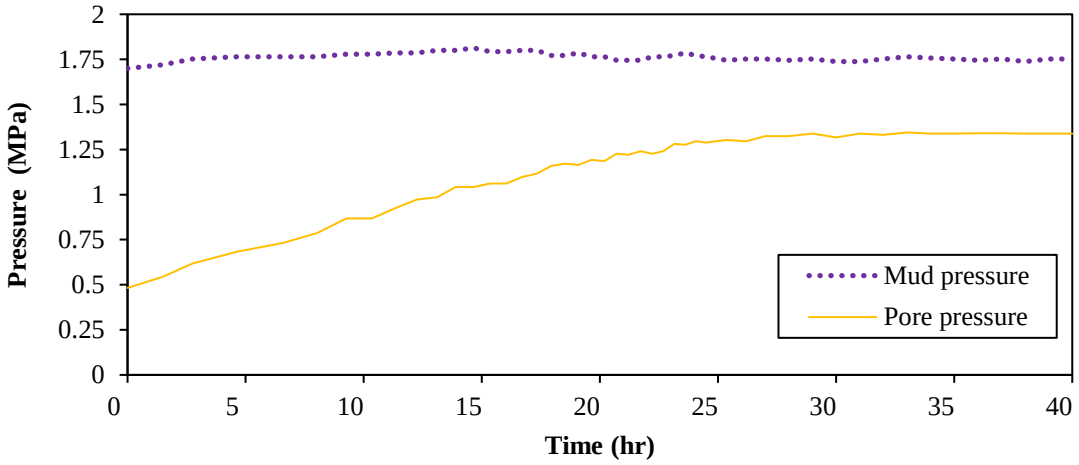

8-a

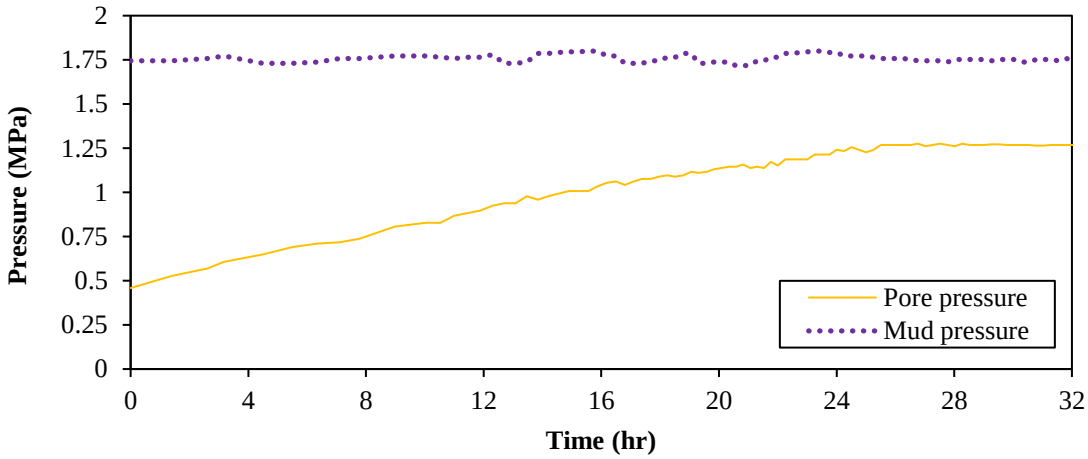

8-b

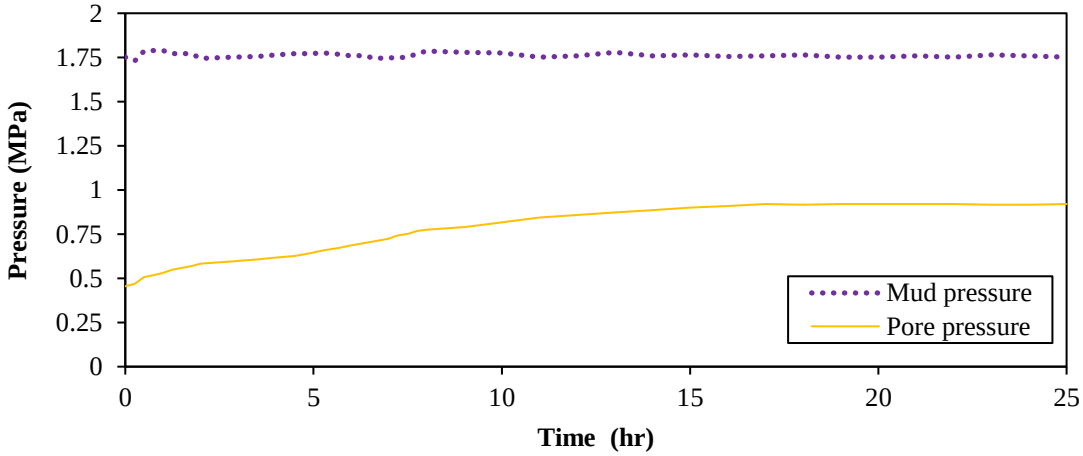

8-c

Figure 8

Results of pore plugging tests of WBDM containing different concentrations of 10 nm nanoparticles in contact with Kazhdumi shale: a) 2 wt.% of nanoparticles; b) NPs; b) 5 wt.% of nanoparticles; c) 10 wt.% of nanoparticles.

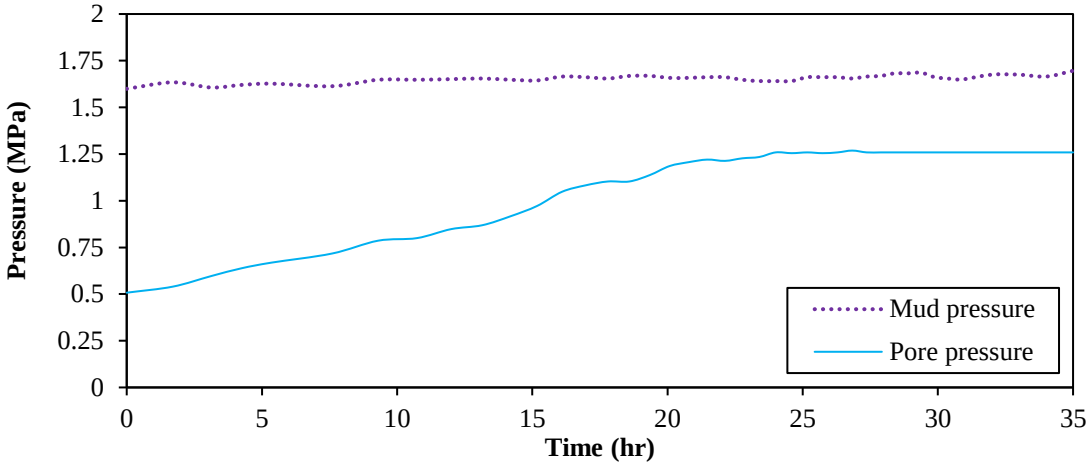

9-a

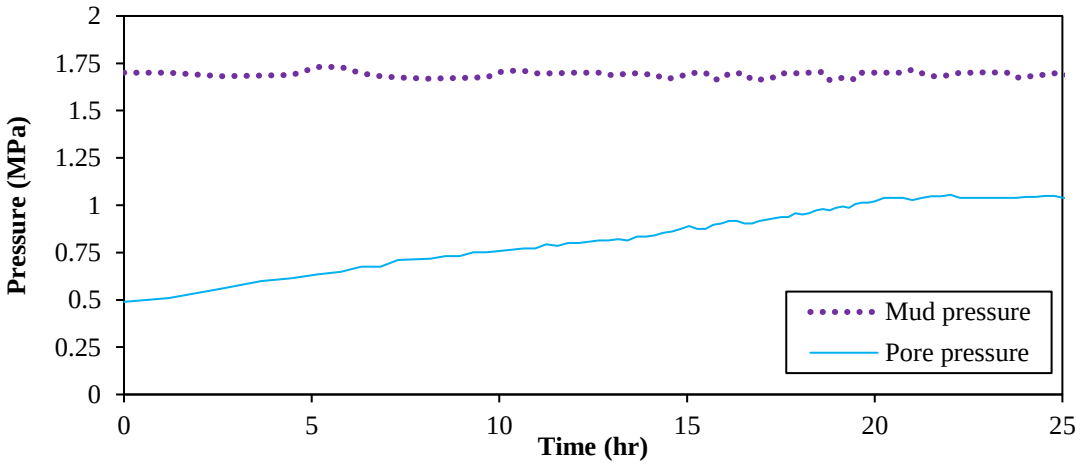

9-b

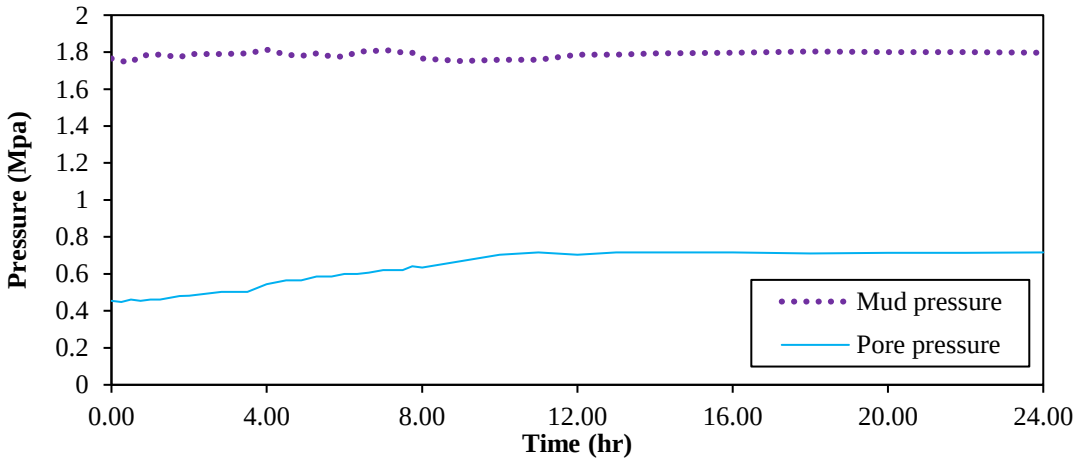

9-c

Figure 9

Results of pore plugging tests of WBDM containing different concentrations of 25 nm nanoparticles in contact with Kazhdumi shale: a) 2 wt.% of nanoparticles; b) 5 wt.% of nanoparticles; c) 10 wt.% of nanoparticles.

When WBDM without nanoparticles was circulating in the mud line to flow across the shale sample, pore pressure built up to 1.2276 MPa after 32 hrs and then leveled off significantly (Figure 7). WBDM is not containing a sealing agent, so a significant reduction in pore pressure build-up rate could be attributed to its viscosity modifier agents such as PHPA, XC-polymer, and PAC-LV. These agents will impart high viscosity to the bulk of the fluid, but they are unable to reduce the viscosity of the filtrate (filtrate viscosity will still be close to the viscosity of water) (Van Oort, 1994). Therefore, it can certainly be claimed that the reduction in pore throats diameter by viscosity agents is responsible for continuing pore pressure build-up rate (Akhtarmanesh et al., 2013). The aforementioned facts could be considered as acceptable reasons for the value of a fractional reduction in pore pressure (0.7515), which is not equal to unity within the test time.

When WBDM contained 2 wt.% (Figure 8-a), 5 wt.% (Figure 8-b), and 10 wt.% (Figure 8-c) 10 nm nanoparticles circulating in the mud line, the pore pressure correspondingly rose to 1.3375 MPa, 1.2686 MPa, and 0.9204 MPa (as plugging pore pressures, Table 5) after 29 hr, 25.5 hrs, and 17 hrs (as plugging times, Figure 10) respectively.

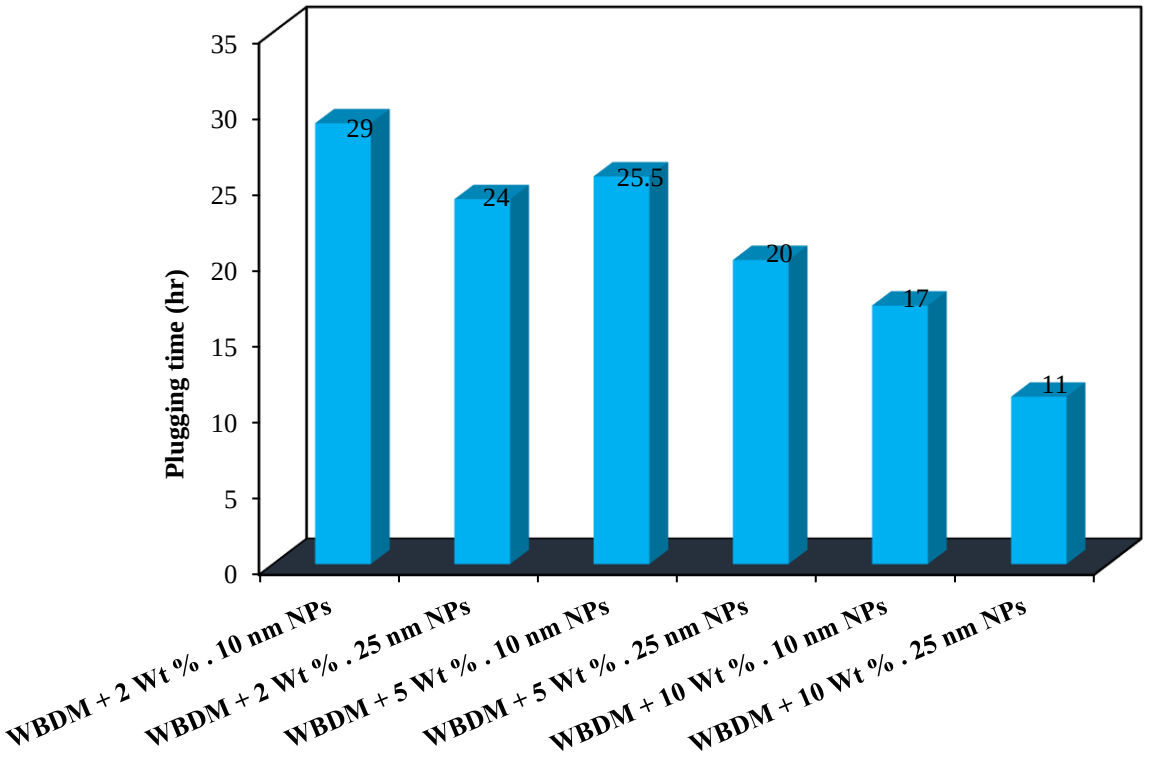

Figure 10
The effect of size and concentration of nanoparticles on the plugging time.

The fluid invasion reduction efficiency was obtained to be 12.17%, 16.86%, and 52.93% respectively for WBDM containing 2 wt.%, 5 wt.%, and 10 wt.% 10 nm nanoparticles (Figure 11). It is clearly evident that an increase in the concentration of nanoparticles decreases pore pressure rate but increases fluid invasion reduction efficiency. The next experiment was investigated using WBDM containing different concentrations of 25 nm nanoparticles. When WBDM contained 2 wt.% (Figure 9-a), 5 wt.% (Figure 9-b), and 10 wt.% (Figure 9-c) of 25 nm nanoparticles circulating in the mud line, the pore pressure correspondingly rose to 1.2589 MPa, 1.0397 MPa, and 0.7163 MPa (as plugging pore pressures, Table 5) after 24 hrs, 20 hrs, and 11 hrs (as plugging times, Figure 10)

respectively. The fluid invasion reduction efficiency was obtained to be 13.47%, 39.49%, and 72.76% respectively for WBDM containing 2 wt.%, 5 wt.%, and 10 wt.% of 25 nm nanoparticles (Figure 11).

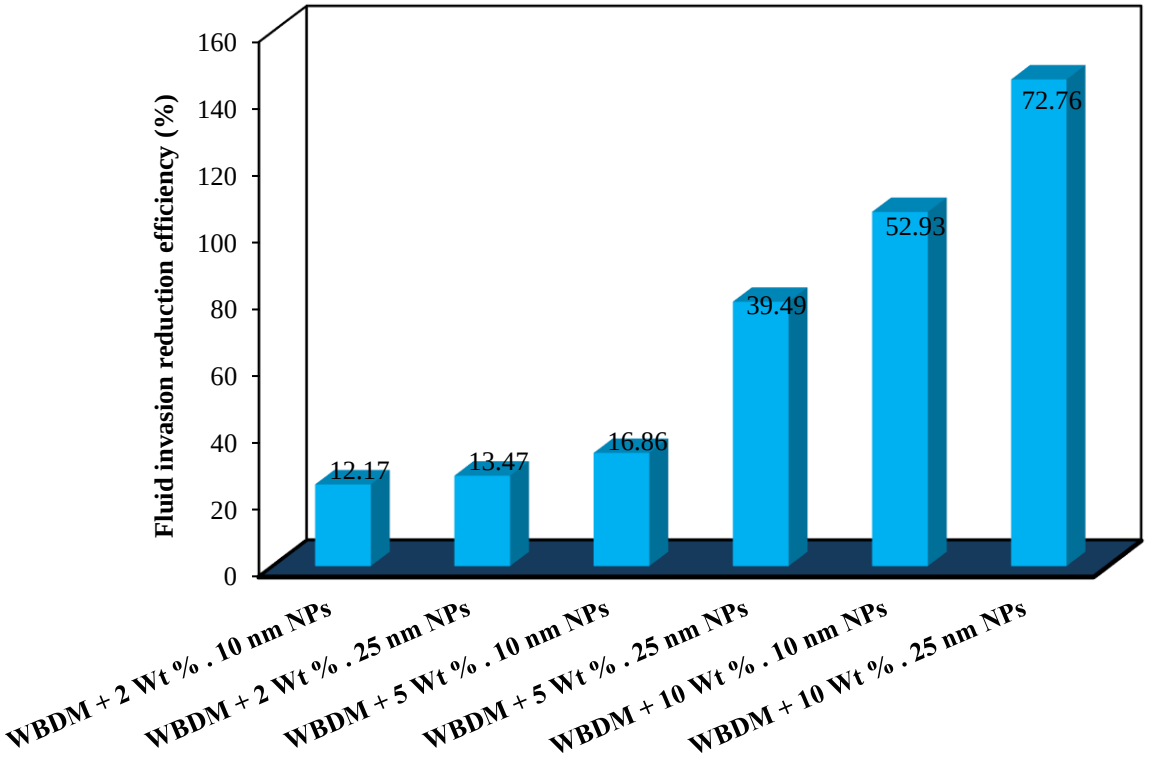

Figure 11
The effect of size and concentration of nanoparticles on the fluid invasion reduction efficiency.

According to the aforementioned discussion, the same trend, which was found for 10 nm nanoparticles, was again observed for 25 nm nanoparticles. Comparing the results obtained for 10 nm and 25 nm nanoparticles, an increase in the size of nanoparticles from 10 nm to 25 nm decreases pore pressure build-up rate (which consequently reduces the plugging time) but improves the fluid invasion reduction efficiency.

Table 5
Recorded pressure data.

Test No.	**1**	**2**	**3**	**4**	**5**	**6**	**7**
Mud type	WBDF	WBDF + 10 nm NPs			WBDF + 25 nm NPs		
NPs (wt.%)	0	2	5	10	2	5	10
IMP (MPa)	1.4996	1.6995	1.7443	1.7512	1.5995	1.6995	1.7650
IPP (MPa)	0.4033	0.4826	0.4585	0.4550	0.5074	0.4895	0.4550
PMP (MPa)	1.4996	1.7512	1.7512	.17581	1.6409	1.6995	1.7581
PPP (MPa)	1.2272	1.3375	1.2686	0.9204	1.2589	1.0397	0.7163
δ_j	0.7515	0.6600	0.6246	0.3537	0.6502	0.4547	0.2047

4. Conclusions

Reducing the fluid invasion into the shale is one of the important factors in shale stability. In this study, the effect of silica nanoparticles, as a physical sealing agent, on the fluid invasion into Kazhdumi shale was investigated. The following 5 conclusions can be drawn based on the results obtained from this study:

1. Kazhdumi shale has a water activity of 0.93, determined using relative humidity measurements;
2. Kazhdumi shale shows very low membrane efficiency (about 1.8%), indicating osmosis phenomenon as an unreliable mechanism for the stability of Kazhdumi shale. Hence avoiding the water invasion into Kazhdumi shale is vital for the stability of this formation during drilling operations;
3. Nanoparticles have a significant positive impact on the water invasion into Kazhdumi shale;
4. For each size (10 nm and 25 nm) of nanoparticles, increasing the nanoparticles concentration from 2 wt.% up to 10 wt.% decreases plugging time but increases fluid invasion reduction efficiency;
5. For each concentration of nanoparticles, increasing the size of nanoparticles from 10 nm to 25 nm decreases plugging time but increases fluid invasion reduction efficiency; for example, in the case of using 10 wt.% of nanoparticles, increasing the size of nanoparticles from 10 nm to 25 nm decreases plugging time from 17 hrs to 11 hrs but increases fluid invasion reduction efficiency from 52.93% to 72.76% respectively.

Acknowledgments

The authors are grateful to the Sahand Petroleum Research Center (SPRC), Petroleum University of Technology (PUT), and National Iranian Drilling Company (NIDC) for their laboratory supports.

Nomenclature

CEC	: Cation exchange capacity
IMP	: Initial mud pressure
IPP	: Initial pore pressure
NPs	: Nanoparticles
OBDM	: Oil-based drilling mud
PAC-LV	: Low viscosity poly anionic cellulose
PHPA	: Partially hydrolyzed polyacrylamide
PMP	: Plugging mud pressure
PPP	: Plugging pore pressure
PT	: Plugging time
WBDM	: Water-based drilling mud
XRD	: X-ray diffraction
Variables	
$\boldsymbol{AV}$	: Apparent viscosity (cP)
$\boldsymbol{A_w}$	: Water activity

$A_{w,porefluid}$	: Water activity of pore fluid
$A_{w,testfluid}$	: Water activity of test fluid
PV	: Plastic viscosity (cP)
R	: Gas constant
T	: Absolute temperature
V	:Partial molar volume of water
YP	: Yield point (Pa)
δ	: Fractional reduction in pressure difference between mud pressure and pore pressure at the initial and plugging times (dimensionless)
δ_B	: Fractional reduction in pressure difference at the initial and plugging times, for base mud (dimensionless)
$\delta_{(B+NPs)_{ii}}$	: Fractional reduction in pressure difference at the initial and plugging time, for base mud incorporated with different concentrations of NPs (ii) (dimensionless)
ΔP	: Measured osmotic pressure (MPa)
ΔP_i	: Pressure difference between the mud pressure and pore pressure at the initial time of test (MPa)
ΔP_p	: Pressure difference between the mud pressure and pore pressure at the plugging time (MPa)
$\Delta\sigma$	: Membrane efficiency (%)
$\Delta\pi$	: Theoretical osmotic pressure (MPa)
ε	: Fluid invasion reduction efficiency (%)
Subscripts	
ii	: Different concentrations of nanoparticles
j	: Different muds

References

Akhtarmanesh, S., Shahrabi, M., and Atashnezhad, A., Improvement of Wellbore Stability in Shale Using Nanoparticles, Journal of Petroleum Science and Engineering, Vol. 112, p. 290-295, 2013.

AL-Bazali, T. M., The Consequences of Using Concentrated Salt Solutions for Mitigating Wellbore Instability in Shales, Journal of Petroleum Science and Engineering, Vol. 80, p.94-101, 2011.

Al-Bazali, T. M., Zhang, J., Chenevert, M. E., and Sharma, M. M., Factors Controlling the Membrane Efficiency of Shales When Interacting with Water-based and Oil-based Muds, International Oil & Gas Conference and Exhibition in China, 2006.

Al-Bazali, T. M., Zhang, J., Chenevert M. E., and Sharma, M. M., A Rapid Rigsite-deployable Electrochemical Test for Evaluating the Membrane Potential of Shales, SPE Drilling & Completion Vol. 22, p. 205-216, 2007.

Anderson, R., Ratcliffe, I., Greenwell, H., Williams, P., Cliffe, S., and Coveney, P., Clay Swelling: a Challenge in the Oilfield, Earth Science Reviews, Vol. 98, p. 201-216, 2010.

API, Recommended Practice Standard Procedure for Field Testing Water-based Drilling Fluids, September, 1997.

Bailey, L., Craster, B., Sawdon, C., Brady, M., and Cliffe, S., New Insight into the Mechanisms of Shale Inhibition Using Water Based Silicate Drilling Fluids, IADC/SPE Drilling Conference, 1998.

Bol, G., Wong, S. W., Davidson, C., and Woodland, D., Borehole Stability in Shales, SPE Drilling & Completion, Vol. 9, p. 87-94, 1994.

Chenevert, M. E., Shale Alteration by Water Adsorption, Journal of Petroleum Technology, Vol. 22, p. 1141-1148, 1970.

Chenevert, M. E. and Sharma, M. M., Maintaining Shale Stability by Pore Plugging, Patent S/N 61/073,679 Filed 06/18/2008.

Diaz-Perez, A., Cortes-Monroy, I., and Roegiers, J., The Role of Water/Clay Interaction in the Shale Characterization, Journal of Petroleum Science and Engineering, Vol. 58, p. 83-98, 2007.

Fam, M. and Dusseault, M., Borehole Stability in Shales: a Physico-chemical Perspective. EUROCK 98. Symposium, 1998.

Hill, D. G., Clay Stabilization Criteria for Best Performance, SPE Formation Damage Control Symposium, 1982.

Lomba, R., Sharma, M. M., and Chenevert, M., Electrochemical Aspects of Wellbore Stability: Ionic Transport through Confined Shales, International Journal of Rock Mechanics and Mining Sciences and Geomechanics Abstracts, 1996.

Lomba, R. F., Chenevert, M., and Sharma, M. M., The Ion-selective Membrane Behavior of Native Shales, Journal of Petroleum Science and Engineering, Vol. 25, p. 9-2, 2000.

Manohar Lal, S. and Amoco, B., Shale Stability: Drilling Fluid Interaction and Shale Strength, SPE Asia Pacific Oil and Gas Conference and Exhibition, 1999.

Mehtar, M. A., Mielke, S. K., Alfonzo, N. E., Young, S., Brangetto, M., and Soliman, A. A., Effective Implementation of High Performance Water-based Fluid Provides Superior Shale Stability Offshore Abu Dhabi, Abu Dhabi International Petroleum Exhibition and Conference, 2010.

Mody, F. K., Tare, U. A., Tan, C. P., Drummond, C. J., and Wu, B., Development of Novel Membrane Efficient Water-based Drilling Fluids through Fundamental Understanding of Osmotic Membrane Generation in Shales, SPE Annual Technical Conference and Exhibition, 2002.

O'Brien, D. E. and Chenevert, M. E., Stabilizing Sensitive Shales with Inhibited Potassium-based Drilling Fluids, Journal of Petroleum Technology, Vol. 25, 1, p. 1089-1100, 1973.

Osuji, C. E., Chenevert, M. E., and Sharma, M. M., Effect of Porosity and Permeability on the Membrane Efficiency of Shales, SPE Annual Technical Conference and Exhibition, 2008.

Patel, A., Stamatakis, S., Young, S., and Friedheim, J., Advances in Inhibitive Water-based Drilling Fluids: Can They Replace Oil-based Muds ?, International Symposium on Oilfield Chemistry, 2007.

Sensoy, T., Chenevert, M. E., and Sharma, M. M., Minimizing Water Invasion in Shales Using Nanoparticles, SPE Annual Technical Conference and Exhibition, 2009.

Steiger, R. P., Fundamentals and Use of Potassium/Polymer Drilling Fluids to Minimize Drilling and Completion Problems Associated with Hydratable Clays, Journal of Petroleum Technology, Vol. 34, p. 1661-1670, 1982.

Steiger, R. P. and Leung, P .K., Quantitative Determination of the Mechanical Properties of Shales, SPE Drilling Engineering, Vol. 7, p. 181-185, 1992.

Tan, C. P., Richards, B. G., and Rahman, S., Managing Physico-chemical Wellbore Instability in Shales with the Chemical Potential Mechanism. SPE Asia Pacific Oil and Gas Conference, 1996.

Van Oort, E., A Novel Technique for the Investigation of Drilling Fluid Induced Borehole Instability in Shales, Rock Mechanics in Petroleum Engineerin, 1994.

Van Oort, E., On the Physical and Chemical Stability of Shales, Journal of Petroleum Science and Engineering, Vol. 38, p. 213-23, 2003.

Van Oort, E., Hale, A., and Mody, F., Manipulation of Coupled Osmotic Flows for Stabilisation of Shales Exposed to Water-based Drilling Fluids, Society of Petroleum Engineers, Annual Technical Conferenc, 1995.

Van Oort, E., Hale, A., Mody, F., and Roy, S., Transport in Shales and the Design of Improved Water-based Shale Drilling Fluids, SPE Drilling & Completion, Vol. 11, p. 137-146, 1996.

Yu, M., Chenevert, M. E., and Sharma, M. M., Chemical–mechanical Wellbore Instability Model for Shales: Accounting for Solute Diffusion, Journal of Petroleum Science and Engineering, Vol. 38, p. 131-143, 2003.

Zeynali, M. E., Mechanical and Physico-chemical Aspects of Wellbore Stability During Drilling Operations, Journal of Petroleum Science and Engineering, Vol. 82, p. 120-124, 2012.

Zhang, S., Qiu, Z., Huang, W., Cao, J., and Luo, X., Characterization of a Novel Aluminum-based Shale Stabilizer, Journal of Petroleum Science and Engineering, Vol. 103, p. 36-40, 2013.

Zhou, Z., Gunter, W., Kadatz, B., and Cameron, S., Effect of Clay Swelling on Reservoir Quality, Journal of Canadian Petroleum Technology, Vol. 35, No. 84, p. 18-23, 1996.

Zhu, X. and Liu, W., The Effects of Drill String Impacts on Wellbore Stability, Journal of Petroleum Science and Engineering, Vol. 109, p. 217-229, 2013.